ACS Macro Letters

Letter

pubs.acs.org/macroletters

Immunoselective Cellulose Nanospheres: A Versatile Platform for Nanotheranostics

Christopher Carrick,*[,†] Lars Wågberg,[†,‡] and Per A. Larsson*[,†]

School of Chemical Science and Engineering, [†]Department of Fibre and Polymer Technology and [‡]Wallenberg Wood Science Center, WWSC, KTH Royal Institute of Technology, SE-100 44 Stockholm, Sweden

Supporting Information

ABSTRACT: This paper describes a novel route for the preparation and functionalization of perfectly spherical cellulose nanospheres (CNSs), ranging from 100 to 400 nm with a typical diameter of 160−170 nm, for use in theranostics. The method of preparation enables both surface and interior bulk functionalization, and this presumably also makes the CNSs suitable for use in end-use applications other than theranostics. Surface functionalization was here demonstrated by antibody conjugation with an antibody specific toward the epidermal growth factor receptor (EGFR) protein, i.e., facilitating interaction with cancer cells having the EGFR. Besides showing specificity, the CNS−antibody conjugates showed a very low nonspecific binding. The CNSs could easily be bulk functionalized by embedding gold nanoparticles in the cellulose sphere matrix during CNS preparation to provide imaging contrast for diagnostic purposes.

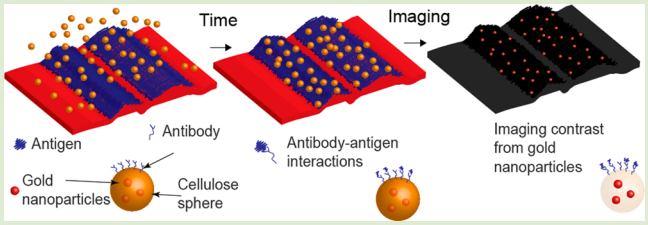

Rapid and precise therapeutic and diagnostic tools are essential for quality of life and to promote human health. In our society, cancer is one of the most common and life-threatening diseases known, and more than 40% of all men and women will one day be diagnosed as having cancer.[1] Several methods are available for diagnosing cancer,[2] and recent studies show that the concentration of the epidermal growth factor receptor (EGFR) protein is much higher in cancer patients than in healthy patients, which makes this protein an interesting target for the fast identification and treatment of patients in the battle against cancer.[3,4]

Several diagnostic tools are available based on specific antigen−antibody, DNA−DNA, or receptor−ligand recognition or interaction, for example, enzyme-linked immunosorbent assay (ELISA).[5] However, conventional ELISA cannot be used in *in vivo* applications since it is limited to external fluid examinations such as a blood sample, and this makes it tedious and labor intense. There is therefore an obvious need for simple and cost-effective analytical tools capable of detecting, locating, and ultimately treating cancer and other diseases *in vivo* at an early stage.

Particle-based assays are rapidly gaining interest since they have shown to be effective for biorecognition without the limitations posed by currently available diagnostic tools, such as that high-throughput screening and multiple receptor and conjugation interactions cannot be studied simultaneously.[6] Micro- and nanoparticle-based systems have a large surface-to-volume ratio and a greater versatility in sample analysis and data acquisition.[7] The particle-based assays can be grouped into two major categories based on particle size: nanoparticles[8] and microparticles.[9] These can further be categorized according to how they provide diagnostic contrast, such as ultrasound,[10] fluorescent markers,[11] dyes,[12] or X-ray scattering.[13] Another contrast agent that has recently gained a lot of interest is gold nanoparticles (GNPs), which can be detected by many different techniques such as surface-enhanced Raman spectroscopy,[14] light microscopy,[11] fluorescent imaging,[11] and enhanced X-ray scatter imaging.[13] GNPs are, unfortunately from a diagnostics point of view, also very potent protein binders, which, due to nonspecificity, limits their use in *in vivo* applications.[15] This problem can be addressed by coating the particles with, for example, polyethylene glycol in order to reduce the interaction with proteins.[4,11,16] Nanoparticles are also affected by aging, having a poorer detection sensitivity already a few days after preparation,[17] which drastically limits their use in clinical implementations. To overcome these shortcomings regarding aggregation, the GNPs can be embedded in larger nano- or submicron particles to provide a protective structure. This protective structure must meet three major criteria: it has to be inert for nonspecific interactions, it must be chemically active to allow for surface modifications to provide specific interactions, and third it is vital that the material does not interfere with the human immune system or human proteins; i.e., it must be biocompatible and not create harmful interactions *in vivo*. One of the most frequently used materials in pharmaceuticals applications that meets all these criteria is cellulose and some of its derivatives,[18,20,21] and it is nowadays commonly used as a drug dispersant or binder.

Received: August 18, 2014
Accepted: October 10, 2014
Published: October 14, 2014

In this work we demonstrate how to prepare and functionalize spherical nanoparticles, cellulose nanospheres (CNSs), which are able to include and stabilize contrast agents such as GNPs and potentially also include therapeutic drugs. The CNSs were prepared by a three-step protocol. In the first step, cellulose (dissolving pulp provided by Domsjö Aditya Birla) was dissolved in lithium chloride in *N*,*N*-dimethylacetamide (LiCl-DMAc).[19] When CNSs with encapsulated GNPs were produced, GNPs from Sigma-Aldrich with a specified diameter of 5 nm (with DLS an average particle size of 9.3 nm was measured) were dispersed in the cellulose solution in the first step. In the second step, the dissolved cellulose was mixed with an immiscible silicone oil (Sigma-Aldrich) at a volume ratio of 1:4, using a vortex mixer to produce an emulsion of micrometer-sized cellulose drops (with or without GNPs) in silicone oil. Finally, in the third step, the emulsion was pushed by pressurized nitrogen through a filter with a pore size of 2 μm (Valco instruments Co. Inc.) into ethanol (i.e., a nonsolvent for cellulose) containing 0.5 wt % Tween 20, forming solidified nanometer-sized cellulose spheres with a high spherical uniformity in contact with the nonsolvent (Figure 1a). To remove larger macroscopic cellulose aggregates formed, due to clogging of filter pores during the cellulose solidification, the dispersion was coarsely filtered through a 5 μm filter (Acrodisc with a Supor membrane). To simulate *in vivo* conditions, the dispersion was solvent-exchanged against 0.14 M pH 7.4 phosphate buffer saline (PBS), using a 1000 kDa dialysis membrane (Biotech CE membrane from Spectrum Laboratories Inc.). This high cutoff also removes nonencapsulated GNPs. The CNSs were then characterized in terms of size and size distribution by scanning electron microscopy (Hitachi S-4800) and dynamic light scattering (DLS) using a Zetasizer ZEN3600 (Malvern Instruments Ltd., U.K.). Both techniques gave a typical sphere diameter of 160−170 nm (Figure 1b and Figure S1, Supporting Information (SI)), which, to the best of our knowledge (excluding nonspherical nanoparticles from cellulose[20]), is about 2 orders of magnitude smaller than any earlier reported values for pure cellulose spheres with high spherical uniformity.[21]

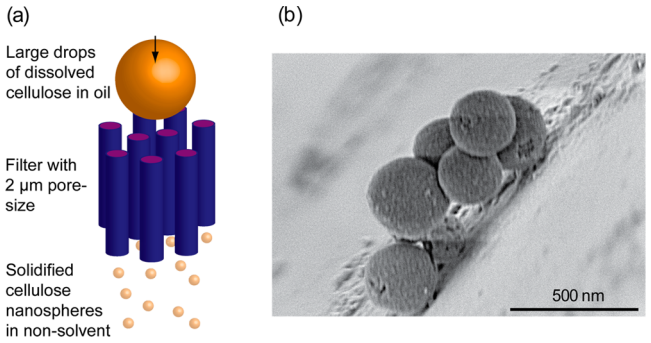

Figure 1. (a) Schematic illustration of how dissolved cellulose droplets in silicone oil are pushed through a 2 μm filter into ethanol where the dissolved cellulose solidifies as CNSs. (b) Scanning electron micrograph of freeze-dried CNS.

Aliquots of the CNS dispersion were then surface functionalized in a three-step antibody conjugation protocol,[22] with dialysis against PBS after each step. First, to enable reaction with the antibody, 5 mL of CNSs dispersed in Milli-Q water was partially oxidized to dialdehyde cellulose for 20 min (60 min was also used but did not affect the conjugation efficiency) by adding 200 μL of 0.5 M sodium periodate solution. After dialysis, 100 μg of antibody, anti-EGFR (Sino Biological Inc.), or anti-BSA (Life technologies) in 1 mL of ten times diluted PBS was added to the oxidized CNSs for 2 h. Finally, to form stable amine bonds between the antibody and CNS and to remove any remaining aldehyde groups, 500 μL of 4 mg/mL of sodium borohydride was added to the mixture. The successful conjugation was supported by DLS size measurements where an increase in the average diameter of the CNS was detected after surface functionalization (see SI). The real-time specificity of the antibody−CNS conjugates was then measured using a quartz crystal microbalance (QCM) of model QCM-E4 (Q-Sense) where the measured shift in frequency is related to the adsorbed mass (for exact experimental details see SI). As can be seen in Figure 2, both the BSA (Figure 2a) and the EGFR (Figure 2b) were adsorbed onto the silica crystal. When the

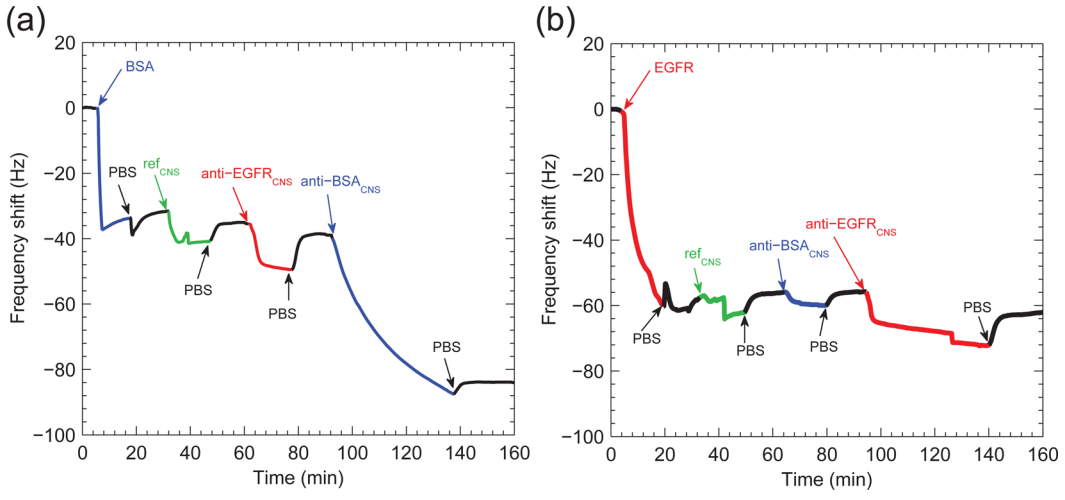

Figure 2. QCM experiments displaying the frequency shift (i.e., mass adsorption) as a function of time. Addition points of protein (BSA or EGFR), washing buffer (PBS), nonconjugated CNSs (ref$_{CNS}$), anti-BSA-CNS conjugated (anti-BSA$_{CNS}$), or anti-EGFR-CNS conjugated (anti-EGFR$_{CNS}$) are indicated by arrows. All CNSs were dispersed in 0.14 M pH 7.4 PBS, and the initial BSA or EGFR layer was adsorbed in the absence of added salt at pH 4 and 5, respectively.

dx.doi.org/10.1021/mz500507k | *ACS Macro Lett.* 2014, 3, 1117−1120

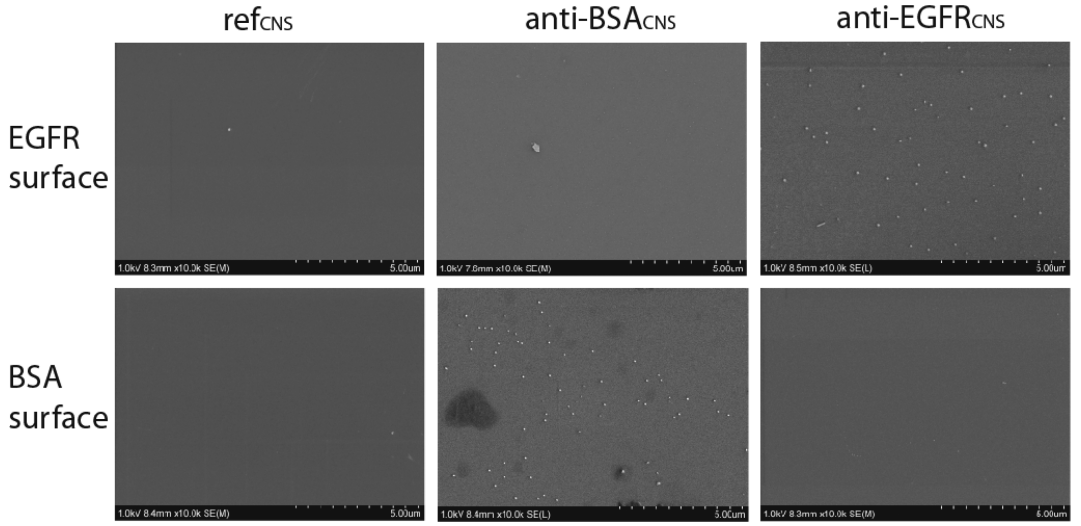

Figure 3. SEM micrographs of EGFR or BSA protein layers adsorbed onto a silica wafer followed by dipping in a solution of ref$_{CNS}$, anti-BSA$_{CNS}$, or anti-EGFR$_{CNS}$. After the adsorption of the different CNSs, the silica plates were washed and freeze-dried to preserve the CNS structure.

nonconjugated CNSs (ref$_{CNS}$) were injected, no significant adsorption to either the BSA or the EGFR-coated surface was detected, and almost all the detected interaction was of a nonspecific type since all immobilized mass (i.e., the entire frequency shift) was removed after PBS washing. The CNS with the "wrong" antibody conjugation showed the same almost complete absence of nonspecific interactions as the ref$_{CNS}$. The spheres with the "right" conjugated antibody showed significant binding to the corresponding protein layer (seen as a higher frequency decrease in Figure 2), and the immobilization continued over a longer period of time than that of the spheres without specific interaction. Equally important, the spheres did not completely detach during the washing step, confirming that they were permanently attached to the protein surface and that the antibody maintained specificity after conjugation with the CNS.

The anti-BSA$_{CNS}$ conjugates were adsorbed more effectively than the anti-EGFR$_{CNS}$ conjugates. The higher adsorption of anti-BSA$_{CNS}$ can presumably be explained by a lower conjugation efficiency, quantified as a conjugation of about 40% for the anti-BSA and about 20% for the anti-EGFR (see SI).

To support the QCM results and to image the absence of nonspecific interactions and the presence of highly specific interactions as observed by QCM, a silica wafer with a preadsorbed protein layer of BSA or EGFR was submerged in test tubes containing each CNS solution (i.e., nonconjugated and conjugated with anti-BSA or anti-EGFR) for 45 min and then washed with PBS for 45 min (Figure 3). The experiment was performed in parallel experiments with each CNS rather than in the sequential series shown in Figure 2. As can be seen in Figure 3, a higher density of immobilized CNS was detected where antibody–antigen interactions were present, in full agreement with the QCM data (Figure 2).

As described earlier, GNPs were loaded into the CNS matrix prior to sphere fabrication in some of the experiments to provide a diagnostic imaging tool. In this work we used X-ray diffraction (XRD) and ultraviolet–visible spectroscopy (UV–vis) to demonstrate successful GNP encapsulation. Figure 4 clearly shows the typical gold crystal peaks at scattering angles of 38, 44, 65, 78, and 82° (the peaks at 36, 42, and 62° correspond to the substrate). The Scherrer equation[23] was used to calculate the average size of the embedded GNPs, which was estimated to be about 12 nm (see SI). The size of the GNPs was further supported by UV–vis where absorption peaks can be seen at approximately 490 and 530 nm (see SI) which are ascribed to the surface plasmon resonance absorption of dispersed GNPs.[24]

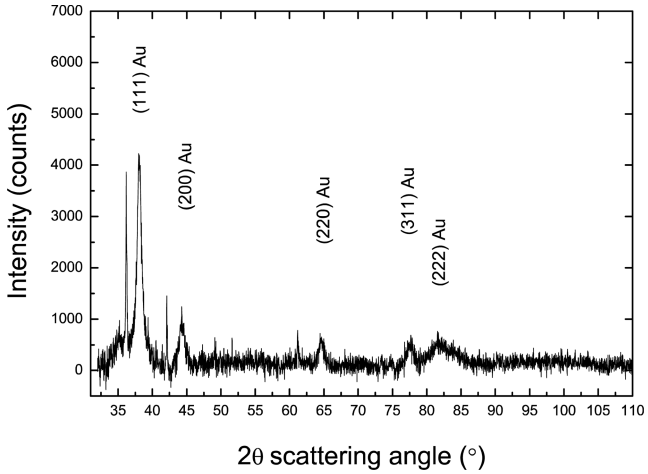

Figure 4. X-ray diffraction of dry, gold-containing CNSs. The labeled peaks at 38, 44, 65, 78, and 82° scattering angles correspond to the different crystalline planes of gold.

Cellulose is one of the most commonly used substrates or dispersants in medical drug treatment. Here we have presented a method of fabricating CNSs that can be both surface and bulk functionalized, and it can be hypothesized that this system may act as an *in vivo* diagnostic tool. As illustrated in Figure 5, the functionalized CNS provides a specific interaction between anomalous cells which can be diagnosed by incorporating a contrast agent such as GNPs. Presumably, also a therapeutic drug could be embedded in the CNS in a manner similar to the incorporation of the GNP, with the goal to locally treat a disease or infection.

In the present paper, the main application of the prepared CNSs has been for the use in theranostics, which we consider to be one of the most interesting applications. However, it must

dx.doi.org/10.1021/mz500507k | *ACS Macro Lett.* 2014, 3, 1117–1120

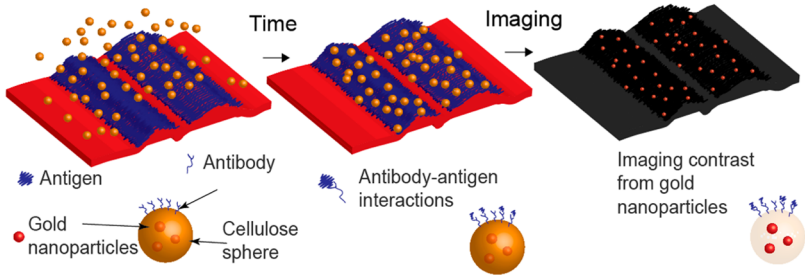

Figure 5. Schematic illustration of how antibody-conjugated CNSs with embedded GNP might be used as an *in vivo* contrast agent to image the specific interactions from antibody conjugation on CNS with antigen present on the surface. In the first image (from the left) is a solution of surface-functionalized CNS injected into an infected location. Subsequently, the functionalized CNSs bind to the antigen surface, where the encapsulated GNPs provide contrast of the infected area.

also be stressed that the technique for the preparation of CNSs, as such, is of broad scientific importance and that the prepared CNSs would be an ideal material for fundamental colloidal studies of cellulose. For example, the influence of steric stabilization and charge interactions can be studied with these particles. Furthermore, by preparing larger particles using larger membranes it should also be possible to prepare new types of colloidal probes for atomic force measurements.

In conclusion, by a membrane emulsification technique cellulose nanospheres with a typical diameter of 160−170 nm have for the first time been prepared. The prepared spheres were then surface functionalized by antibody conjugation to provide specific antibody−antigen interactions with simultaneous low nonspecific interactions. It was also possible to bulk functionalize the cellulose nanospheres by incorporating GNPs to provide a diagnostic tool for cancer cells containing EGFR.

■ ASSOCIATED CONTENT

Supporting Information

Additional information and figures. This material is available free of charge via the Internet at http://pubs.acs.org.

■ AUTHOR INFORMATION

Corresponding Authors

*E-mail: ccarrick@kth.se.

*E-mail: per.larsson@polymer.kth.se.

Notes

The authors declare no competing financial interest.

■ ACKNOWLEDGMENTS

We thank Dr. Inna Soroka for generous help regarding the XRD experiment. Lars Wågberg gratefully acknowledges funding from the Wallenberg Wood Science Center, and Per Larsson acknowledges the financial support from the BiMaC Innovation research centre at KTH.

■ REFERENCES

(1) Howlader N. N. A.; Krapcho, M.; Garshell, J.; Neyman, N.; Altekruse, S. F.; Kosary, C. L.; Yu, M.; Ruhl, J.; Tatalovich, Z.; Cho, H.; Mariotto, A.; Lewis, D. R.; Chen, H. S.; Feuer, E. J.; Cronin K. A. National Cancer Institute: Surveillance, Epidemiology, and End Results. *SEER Cancer Statistics Review 1975−2010*, 2013. Available: http://seer.cancer.gov/csr/1975_2010/results_single/sect_01_table12_2pgs.pdf.

(2) Henschke, C. I.; McCauley, D. I.; Yankelevitz, D. F.; Naidich, D. P.; McGuinness, G.; Miettinen, O. S.; Libby, D. M.; Pasmantier, M. W.; Koizumi, J.; Altorki, N. K.; Smith, J. P. *Lancet* **1999**, *354*, 99−105.

(3) Kuan, C. T.; Wikstrand, Cj; Fau - Bigner, D. D.; Bigner, D. D. *Endocr.-Relat. Cancer* **2001**, *8*, 86−93.

(4) Perrault, S. D.; Chan, W. C. W. *Proc. Natl. Acad. Sci. U.S.A.* **2010**, *107*, 11194−11199.

(5) Khan, J.; Brennan, D. M.; Bradley, N.; Gao, B. R.; Bruckdorfer, R.; Jacobs, M. *Biochem. J.* **1998**, *330*, 795−801.

(6) Garcia, J. M.; Gao, A.; He, P. L.; Choi, J.; Tang, W.; Bruzzone, R.; Schwartz, O.; Naya, H.; Nan, F. J.; Li, J.; Altmeyer, R.; Zuo, J. P. *Antiviral Res.* **2009**, *81*, 239−247.

(7) Qian, X.; Peng, X.-H.; Ansari, D. O.; Yin-Goen, Q.; Chen, G. Z.; Shin, D. M.; Yang, L.; Young, A. N.; Wang, M. D.; Nie, S. *Nat. Biotechnol.* **2008**, *26*, 83−90.

(8) Wang, Y.; Liu, Y.; Luehmann, H.; Xia, X.; Wan, D.; Cutler, C.; Xia, Y. *Nano Lett.* **2013**, *13*, 581−585.

(9) Zhang, F.; Haushalter, R. C.; Haushalter, R. W.; Shi, Y.; Zhang, Y.; Ding, K.; Zhao, D.; Stucky, G. D. *Small* **2011**, *7*, 1972−1976.

(10) Klibanov, A. L. *Adv. Drug Delivery Rev.* **1999**, *37*, 139−157.

(11) Conde, J.; Rosa, J.; de la Fuente, J.; Baptista, P. *Biomaterials* **2013**, *34*, 2516−2523.

(12) Zhao, X.-W.; Liu, Z.-B.; Yang, H.; Nagai, K.; Zhao, Y.-H.; Gu, Z.-Z. *Chem. Mater.* **2006**, *18*, 2443−2449.

(13) Rand, D.; Ortiz, V.; Liu, Y.; Derdak, Z.; Wands, J. R.; Tatíček, M.; Rose-Petruck, C. *Nano Lett.* **2011**, *11*, 2678−2683.

(14) Wang, X.; Qian, X.; Beitler, J. J.; Chen, Z. G.; Khuri, F. R.; Lewis, M. M.; Shin, H. J. C.; Nie, S.; Shin, D. M. *Cancer Res.* **2011**, *71*, 1526−1532.

(15) Lacerda, S. H. D. P.; Park, J. J.; Meuse, C.; Pristinski, D.; Becker, M. L.; Karim, A.; Douglas, J. F. *ACS Nano* **2009**, *4*, 365−379.

(16) Dai, Q.; Walkey, C.; Chan, W. C. W. *Angew. Chem., Int. Ed.* **2014**, *53*, 5093−5096.

(17) Vangala, K.; Ameer, F.; Salomon, G.; Le, V.; Lewis, E.; Yu, L.; Liu, D.; Zhang, D. *J. Phys. Chem. C* **2012**, *116*, 3645−3652.

(18) Taajamaa, L.; Rojas, O. J.; Laine, J.; Yliniemi, K.; Kontturi, E. *Chem. Commun.* **2013**, *49*, 1318−1320.

(19) Berthold, F.; Gustafsson, K.; Berggren, R.; Sjöholm, E.; Lindström, M. *J. Appl. Polym. Sci.* **2004**, *94*, 424−431.

(20) Zhang, J.; Elder, T. J.; Pu, Y.; Ragauskas, A. J. *Carbohydr. Polym.* **2007**, *69*, 607−611.

(21) Stiernstedt, J.; Nordgren, N.; Wågberg, L.; Brumer Iii, H.; Gray, D. G.; Rutland, M. W. *J. Colloid Interface Sci.* **2006**, *303*, 117−123.

(22) Wisdom, G. B. *Immunochemical Protocols*; Burns, R., Ed.; Humana Press: Totowa, NJ, 2005; Vol. *295*, pp 127−130.

(23) Scherrer, P. *Nachr. Ges. Wiss. Göttingen, Math.-Phys. Kl.* **1918**, 98−100.

(24) Zhang, F. X.; Han, L.; Israel, L. B.; Daras, J. G.; Maye, M. M.; K. Ly, N.; Zhong, C. J. *Analyst* **2002**, *127*, 462−465.